

Virtual Sequential Picture for Nonsequential Two-Photon Double Ionization of Helium

Wei-Chao Jiang,¹ Jun-Yi Shan,¹ Qihuang Gong,^{1,2} and Liang-You Peng^{1,2,*}

¹State Key Laboratory for Mesoscopic Physics and Department of Physics, Peking University, Beijing 100871, China

²Collaborative Innovation Center of Quantum Matter, Beijing 100871, China

(Received 18 May 2015; published 8 October 2015)

By using a model based on the second-order time-dependent perturbation theory, we show that the nonsequential two-photon double ionization of He can be understood in a virtual sequential picture: to excite the final double continuum state $|\mathbf{k}_1, \mathbf{k}_2\rangle$ by absorbing two photons from the ground state $|1s^2, ^1S_0\rangle$, the single continuum states $|1s, \mathbf{k}_1\rangle$ and $|1s, \mathbf{k}_2\rangle$ serve as the dominant intermediate states. This virtual sequential picture is verified by the perfect agreement of the total ionization cross section, respectively, calculated by this model and by the sophisticated numerical solution to the full-dimensional time-dependent Schrödinger equation. This model, without the consideration of the electron correlation in the final double continuum state, works well for a wide range of laser parameters extending from the nonsequential to the sequential regime. The present Letter demonstrates that the electron correlation in the final double continuum state is not important in evaluating the total cross section, while it is indispensable for an accurate computation of a triply differential cross section. In addition, the virtual sequential picture bridges the sequential and nonsequential two-photon double ionization and reveals connections and distinctions between them.

DOI: 10.1103/PhysRevLett.115.153002

PACS numbers: 32.80.Rm, 32.80.Fb, 42.50.Hz

The helium atom is an ideal object for the study of the quantum three-body problem, which turns out to be a great challenge for the theoretical description [1,2]. In the double ionization of He, both the two electrons are driven to the continuum for which an accurate description is still lacking [3]. In fact, quantum mechanics does not provide any analytical wave functions for systems of no less than three particles. If we artificially neglect or weaken the electron correlation term $1/r_{12} = 1/(\mathbf{r}_1 - \mathbf{r}_2)$ (atomic units are used throughout unless otherwise stated), the two-electron wave functions can be expressed as a product of one-electron wave functions. In this case, the laser induced double ionization can usually be understood as a sequential picture which can be useful in explaining many double-ionization phenomena. In the sequential double-ionization picture of He, one electron is first ejected from the neutral atom leaving the second electron in the ground state of He^+ , from which the second electron is subsequently ejected. However, the existence of the electron correlation may lead to the breakdown of the sequential picture. In the past twenty years, much attention has been paid to nonsequential double ionization [4], whose description is beyond the sequential picture.

In the double ionization of atoms by strong IR laser pulses [5–7], it has been widely accepted that the nonsequential double ionization can be interpreted as a rescattering mechanism [8], in which an approximate classical treatment of the electron motion has been shown to be helpful in the theoretical analysis. However, in the region of extreme-ultraviolet laser pulses, double ionization of He can take place by absorbing a few photons, and the

approximate classical treatment of the electron motion seems helpless. The one-photon double ionization of He is the most fundamental double-ionization process and has been well understood after many years of great efforts [9–11]. However, the two-photon double ionization (TPDI) is much less understood. The developments of the free-electron laser [12–14] and the high-order harmonics [15,16] laser sources provide the possibility to experimentally study the nonlinear TPDI of He, which has continuously attracted a large amount of interest.

The TPDI of He can be sequential if the photon energy ω is larger than the ionization potential of He^+ (54.4 eV), i.e., $\text{He} + \omega \rightarrow \text{He}^+ + e^-$ and then, $\text{He}^+ + \omega \rightarrow \text{He}^{2+} + e^-$. Such a sequential picture breaks down if $39.5 \text{ eV} < \omega < 54.4 \text{ eV}$, in which case TPDI can still happen [17]. In this Letter, we show that even the nonsequential TPDI in the latter case can be described by a virtual sequential picture, which allows us to accurately extract the total cross section (TCS) of the nonsequential TPDI even when the electron correlation in the relevant two-electron wave functions is largely neglected.

The TCS is one of the most basic physical quantities to describe the nonsequential TPDI process. A large number of sophisticated calculations have been performed to estimate the TCS of the nonsequential TPDI, but an indubitable conclusion has not yet been drawn [4]. Theoretical debates focus on the role of the electron correlation in the double continuum state, and existing experimental measurements cannot make a final judgement due to the large uncertainty in evaluating the laser pulse peak intensity, pulse shape, and pulse duration [12,15,16].

Many calculations take the strategy of numerically solving the time-dependent Schrödinger equation (TDSE), in which the TCS is obtained by projecting the final wave function to the double continuum [18–25]. Some calculations, including multichannel theory [26,27] and the J -matrix method [28], indicate that the electron correlation in the double continuum is essential to the TCS of the nonsequential TPDI, while the other calculations, including external complex scaling [29–32], convergent close coupling (CCC) [33–35], R -matrix theory [36,37], and treatment of the electron correlation as a perturbation to obtain the double continuum [24], support an opposite view. This divergence makes the nonsequential TPDI even more mysterious.

The calculation based on the lowest order perturbation theory (LOPT) [26,32,34,35,38–40] has also been performed to obtain the TCS. Usually, the double continuum as the final state is necessary in the LOPT calculations. In the early LOPT calculation for the TCS [38], the electron correlation in the double continuum is completely neglected. However, the TCS obtained in that calculation is much lower than the later sophisticated calculations. One may attribute this failure to the neglect of the electron correlation in the double continuum, but one will see that this is unfair. We use a model based on the second-order time-dependent perturbation theory (TDPT) to calculate the TCS. In the TDPT model, the electron correlation in the double continuum is also completely neglected. This TDPT model was previously developed to explain the sequential TPDI [41–46], but it does not predict zero signal in the nonsequential photon region. To apply the TDPT model to the nonsequential TPDI, we are also inspired by another two works: one is the TDSE calculations performed by Pazourek *et al.* [47], who showed that the sequential TPDI and nonsequential TPDI have universal features; the other one is the time-independent model reported by Fjørre *et al.* [48], who provided a simple formula to reproduce the TCS.

In the present TDPT model, after the integration of angles in the two-electron momentum space, the joint energy spectrum of the two electrons is given by [41]

$$P(E_1, E_2) = \frac{1}{2} \left(\frac{c}{4\pi^2} \right)^2 \left| \sqrt{\frac{\sigma^{\text{He}}(E_1)}{\omega_{ai}}} \sqrt{\frac{\sigma^{\text{He}^+}(E_2)}{\omega_{fa}}} K(E_a) + \sqrt{\frac{\sigma^{\text{He}}(E_2)}{\omega_{bi}}} \sqrt{\frac{\sigma^{\text{He}^+}(E_1)}{\omega_{fb}}} K(E_b) \right|^2, \quad (1)$$

where E_1 and E_2 are the energies of the two electrons, c is the speed of light, $\sigma^{\text{He}}(E)$ and $\sigma^{\text{He}^+}(E)$ are, respectively, the one-photon single-ionization cross section of He and He^+ [49], $\omega_{ai} = E_a - E_i$, $\omega_{fa} = E_f - E_a$, $\omega_{bi} = E_b - E_i$, $\omega_{fb} = E_f - E_b$, $E_i = -2.9037$, $E_a = E_1 - 2.0$, $E_b = E_2 - 2.0$, $E_f = E_1 + E_2$, and the function $K(E_a)$ is given by

$$K(E_a) = \int_{-\infty}^{\infty} d\tau_1 F(\tau_1) e^{i\omega_{fa}\tau_1} \int_{-\infty}^{\tau_1} d\tau_2 F(\tau_2) e^{i\omega_{ai}\tau_2}, \quad (2)$$

where $F(t)$ is the electric field of the laser pulse. Replacing the subscript a by b in Eq. (2), one immediately obtains $K(E_b)$. The total probability for double ionization is given by $P_{\text{total}} = \iint P(E_1, E_2) dE_1 dE_2$, and the TCS is evaluated by $\sigma = (\omega/I_0)^2 (P_{\text{total}}/T_{\text{eff}})$, where I_0 is peak intensity of the laser pulse and T_{eff} is an effective pulse length given by $T_{\text{eff}} = \int_{-\infty}^{\infty} f^4(t) dt$, with $f(t)$ being the envelope of the laser pulse. For the \sin^2 envelope used presently, $T_{\text{eff}} = 35T/128$, where T is the total pulse duration.

In Figs. 1(a) and 1(b), one can see that, in the whole nonsequential regime, the TDPT model nicely reproduces the TCS from the TDSE calculations by Pazourek *et al.* [47] for different pulse durations: 1, 4, 11, and 20 fs. The pulse duration of 20 fs [green solid circles in Fig. 1(b)] reported by Pazourek *et al.* [47] is the longest laser pulse ever used in the TDSE calculation of the TCS, as far as we know. Compared with the time-independent model [48] given by Fjørre *et al.* [small black solid circles in Fig. 1(b)], the result from the present TDPT model is closer to that of the TDSE calculation for 20 fs. In the TDPT model, changing the pulse duration from 20 to 100 fs, the TCSs at the photon energy of 53.5 and 54 eV do not change significantly, i.e., it does not make the present TDPT model closer to the time-independent model of Fjørre *et al.* [48].

The cross section is defined for the ideal infinitely long pulse. It is possible to obtain the long pulse limit of the present TDPT model, in which case the singly differential cross section will be given by

$$\frac{d\sigma}{dE_1} = \frac{\omega^2}{4\pi} |F_1 + F_2|^2, \quad (3)$$

$$F_1 = \sqrt{\frac{\sigma^{\text{He}}(E_1)\sigma^{\text{He}^+}(E_2)}{\omega_{ai}\omega_{fa}}} \frac{1}{\omega_{ai} - \omega}, \quad (4)$$

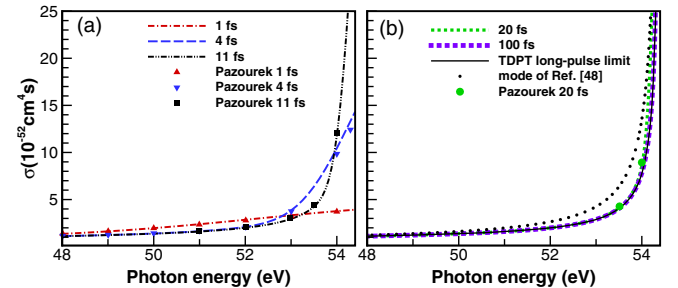


FIG. 1 (color online). TCS of the nonsequential TPDI. (a) The TDPT model calculations (lines labeled by the pulse duration) are compared with the TDSE calculations by Pazourek *et al.* [47] (large symbols). In the right panel (b), the black solid line is the infinitely long pulse limit of the TDPT model [see Eq. (3)]; the small solid circles are the results calculated according to the time-independent model provided by Fjørre *et al.* [48].

$$F_2 = \sqrt{\frac{\sigma^{\text{He}}(E_2)\sigma^{\text{He}^+}(E_1)}{\omega_{bi}\omega_{fb}}} \frac{1}{\omega_{bi} - \omega}, \quad (5)$$

where $E_1 + E_2 = 2\omega - 2.9037$. The TCS for the infinitely long pulse limit is given as the black solid line in Fig. 1(b). One can see that the TCSs for the 20 and 100 fs pulses, indeed, approach the present long pulse limit, rather than the time-independent model of Førre *et al.* The singly differential cross section from the time-independent model of Førre *et al.* can be expressed as [48]

$$\frac{d\sigma}{dE_1} = \frac{\omega^2}{2\pi} (F_1^2 + F_2^2). \quad (6)$$

Equation (6) is identical to Eq. (3) in the case of $F_1 = F_2$, while, in other cases, Eq. (6) always predicts larger values than that of Eq. (3). For the photon energy far from the sequential threshold, one actually has $F_1 \approx F_2$, thus, the time-independent model of Førre *et al.* is equivalent to ours. Similar expressions were also reported in Refs. [43,45]. The result given by Eq. (8) in Ref. [43], which can be obtained by setting $\omega_{ai}\omega_{fa} \approx \omega_{bi}\omega_{fb} \approx \omega^2$ in Eq. (3), is actually smaller than that from the above Eq. (3).

For the second-order perturbation calculation, besides the intractable problem of the electron correlation, another challenge is to handle an infinite number of intermediate states. In the early LOPT calculation [38], several singly excited bound states $|1snp\rangle$ were chosen to be the dominant intermediate states. We assert that this approximation, rather than the neglect of the electron correlation in the double continuum, leads to the failure in the calculation of the TCS. In the present TDPT model, the singly ionized continuum states $|1s, \mathbf{k}_1\rangle$ and $|1s, \mathbf{k}_2\rangle$ are assumed to be the dominant intermediate states which lead to the excitation of the double continuum state $|\mathbf{k}_1, \mathbf{k}_2\rangle$. This assumption is widely taken in the sequential TPDI [42–46,50], since it obviously corresponds to the real sequential picture. Here, we have seen that an assumption of a virtual sequential picture is also valid for the nonsequential TPDI.

The present model can address the physical connections and distinctions between the sequential and nonsequential TPDI. The deep connection between the two processes is that they have the same kind of intermediate states, i.e., the singly ionized continuum states. For this reason, the two TPDI processes have many common features [47]. It can be mathematically proven that the transition matrix from the other intermediate states, except the single-ionization continuum to the double-ionization continuum, will be zero in the condition that the electron correlation is completely neglected. This conclusion may explain why single-ionization continuum states are dominant. Given this deep connection between the sequential TDPI and the nonsequential TPDI, one might not be too surprised at the success on the TCS of the present model. The distinction

between the two TPDI is whether resonances can actually happen or not. For the sequential TPDI, the sequential peaks ($E_1 = \omega - 0.9037$ a.u., $E_2 = \omega - 2.0$ a.u.) in the energy spectrum, in fact, correspond to resonances, i.e., the energy difference between the intermediate states and the final states and the energy difference between the ground state and the intermediate states happen to be the energy of the incident photon. In this resonance case, the denominator in Eq. (4) or Eq. (5) can be zero, which makes it impossible to define the cross section for the sequential TPDI. However, such resonances will never actually happen in the nonsequential TPDI.

To show that the TDPT model can uniformly describe the sequential and nonsequential TPDI, we extend the photon energy above the sequential threshold to calculate the TCS. In Fig. 2, we compare results from the TDPT model with those of TDSE calculations, whose methodologies have been reported previously [41,50–52]. Again, one finds perfect agreement in the sequential regime for different pulse durations. For the sequential TPDI, the TCS is not a well-defined physical quantity; since the total double-ionization probability is proportional to the square of the pulse duration, the TCS is proportional to the pulse duration and will not converge to a finite value as the laser pulse is increased.

For the crossover from the nonsequential to the sequential TPDI, the TCS shows a sharp rise [19,32,53], and extremely long laser pulses are needed to extract a convergent TCS. In the numerical TDSE calculations, it is a daunting task to study the pulse-duration dependence for the two-photon absorption very close to the sequential threshold. In Fig. 3, we show the predictions from the TDPT model in the photon energy region 54.0–54.4 eV, which is close to the sequential threshold. In this photon energy region, there are obviously visible pulse-duration dependences even for the laser pulses longer than 20 fs. The TCS extracted from the 1000 fs laser pulse does approach the long pulse limit. Also, one can see that the predictions

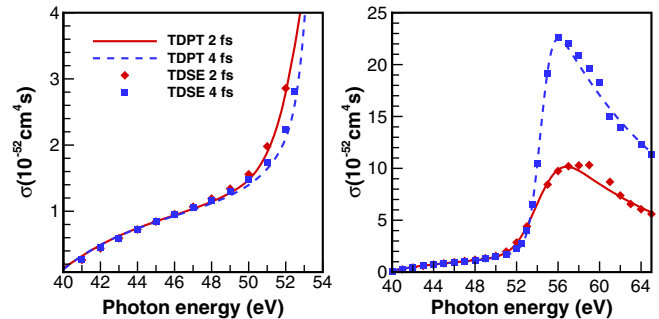


FIG. 2 (color online). Similar to Fig. 1, and the photon energy is increased above the sequential ionization threshold of 54.4 eV. The results of the TDPT model (lines) are compared with those of the TDSE calculations (symbols). The left panel is an enlarged version for part of the right panel.

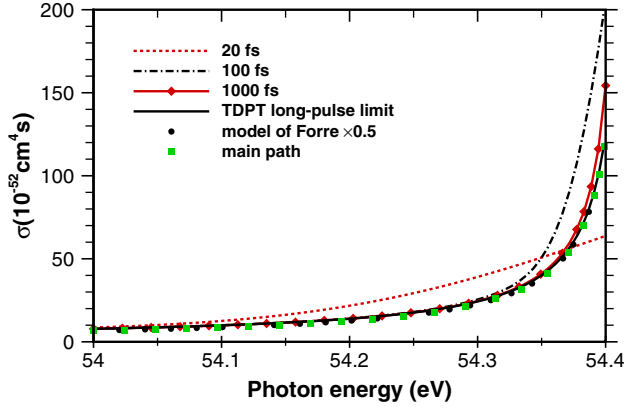


FIG. 3 (color online). Similar to Fig. 1 but for photon energy close to the sequential threshold. The symbols or lines labeled by the pulse duration are the results from the TDPT model. The black solid line is the infinitely long pulse limit of the TDPT model [see Eq. (3)]. The black solid circles are the results from the time-independent model [48] of Førré *et al.* [see Eq. (6)], which have been divided by two. The green solid squares are the results from the infinitely long pulse limit calculation by only including one of the most dominated ionization paths, see the text for details.

from the time-independent model of Førré *et al.* [48] is exactly twice of the present long pulse limit. This is because that the contributions from two ionization paths via $|1s, \mathbf{k}_1\rangle$ and $|1s, \mathbf{k}_2\rangle$ are extremely unequal. Let us mark the electron with the smaller energy as $\mathbf{k}_<$ and the larger one as $\mathbf{k}_>$. In the case that $|\mathbf{k}_<|$ is much smaller than $|\mathbf{k}_>|$, the transition from the ground state to $|1s, \mathbf{k}_>\rangle$ and the transition from the $|1s, \mathbf{k}_>\rangle$ to the double continuum $|\mathbf{k}_<, \mathbf{k}_>\rangle$ is near resonant, i.e., the photon energy is quite close to the energy difference between the relative two states. Thus, the contribution of the intermediate state $|1s, \mathbf{k}_>\rangle$ can be extremely large. This explains the sharp rise of the TCS [19,32,53] and the extremely unequal energy sharing between the two ejected electrons [21] near the sequential threshold. Since the ionization path via $|1s, \mathbf{k}_>\rangle$ is much more important than the one via $|1s, \mathbf{k}_<\rangle$, we can neglect the less important one in our model calculation. Then the long pulse limit Eq. (3) can be reduced to $(d\sigma/dE_1) = (\omega^2/4\pi)F_>^2$, while the time-independent model of Førré *et al.* Eq. (6) can be reduced to $(d\sigma/dE_1) = (\omega^2/2\pi)F_>^2$, where $F_>$ corresponds to the ionization path via $|1s, \mathbf{k}_>\rangle$. Now, the origin of the difference between these two models becomes clear. The calculation that only includes the dominated ionization path ($(d\sigma/dE_1) = (\omega^2/4\pi)F_>^2$) is shown in Fig. 3 as green solid squares, which also agrees well with the long pulse limit (black solid line). One should note that the double ionization can be more complex for photon energy very close to the threshold, since the two-photon excitation-plus-ionization process of the Rydberg series, which is beyond the present model, may contribute to the two-electron ejection [40].

In the perturbation calculations, the requirement for the electron correlation in the double continuum can be more strict than that in the TDSE calculation, because, in the latter case, the effect of the electron correlation in the double continuum can be largely reduced by a sufficiently long free propagation of the final wave function [47]. Though the utilization of the uncorrelated double continuum leads to rather “accurate” results of TCS, the present TDPT fails in the prediction of the triply differential cross section (TDCS). In the TDPT model, the angular distributions of the two electrons simply depend on $\cos^2 \theta_1 \cos^2 \theta_2$, which is obviously insufficient to describe those TDCSs reported from TDSE calculations [20]. It seems that the effect of the electron correlation for the two-photon double ionization can be divided into two steps: in the first step, the two electrons decide to overcome the bounding of the nucleus, and the main role of the electron correlation is to reduce the double-ionization potential; in the second step, the two electrons gradually leave the nucleus and the electron correlation will significantly change the ejection directions of the two electrons but without changing the total ionization probability any more. Our present model can describe “the first step” but fail in “the second step,” for which the inclusion of the electron correlation in the double continuum would be indispensable.

In summary, we assume that the single continuum states $|1s, \mathbf{k}_1\rangle$ and $|1s, \mathbf{k}_2\rangle$ are the dominant intermediate states for the excitation of the double continuum $|\mathbf{k}_1, \mathbf{k}_2\rangle$ in the two-photon double ionization of the ground-state He. This assumption corresponds to a virtual sequential picture, which can universally describe the sequential and non-sequential TPDI. Further, by completely neglecting the electron correlation in the final double continuum and intermediate single continuum, the “accurate” TCS can be obtained. The dependence of the TCS on the pulse duration in the TDSE calculations can be perfectly reproduced by the present TDPT model. For photon energy far from (much smaller than) the sequential threshold, the contributions from the two intermediate single continuums are approximately equal in the calculation of the TCS. Nevertheless, for photon energy around the sequential threshold, TPDI is dominated by the ionization path via the single continuum that corresponds to the release of the high energy one of the two electrons. The connections and distinctions between the long pulse limit of the present TDPT model and the time-independent model of Førré *et al.* [48] are also analyzed. This Letter advances new understanding of the TPDI of He and calls attention to more reliable experimental measurements. Combining the present idea of the virtual sequential picture with those sophisticated methods which aim to address the electron correlation in the double continuum such as the CCC method [33–35] and the three-body Coulomb wavefunction method [54–57], one may obtain reasonable angular distributions of the two ejected electrons in TPDI.

This work is supported by the National Natural Science Foundation of China (NNSFC) under Grant No. 11322437, by the National Program on Key Basic Research Project (973 Program) under Grant No. 2013CB922402, by NNSFC under Grants No. 11174016, and No. 11121091, and by the Program for New Century Excellent Talents in University (NCET).

*liangyou.peng@pku.edu.cn;

<http://www.phy.pku.edu.cn/~lypeng/>

- [1] G. Tanner, K. Richter, and J. Rost, *Rev. Mod. Phys.* **72**, 497 (2000).
- [2] P. Lambropoulos, P. Maragakis, and J. Zhang, *Phys. Rep.* **305**, 203 (1998).
- [3] C. McCurdy, M. Baertschy, and T. Rescigno, *J. Phys. B* **37**, R137 (2004).
- [4] L.-Y. Peng, W.-C. Jiang, J.-W. Geng, W.-H. Xiong, and Q. Gong, *Phys. Rep.* **575**, 1 (2015).
- [5] W. Becker, X. J. Liu, P. J. Ho, and J. H. Eberly, *Rev. Mod. Phys.* **84**, 1011 (2012).
- [6] C. F. d. M. Faria and X. Liu, *J. Mod. Opt.* **58**, 1076 (2011).
- [7] W. Becker and H. Rottke, *Contemp. Phys.* **49**, 199 (2008).
- [8] P. B. Corkum, *Phys. Rev. Lett.* **71**, 1994 (1993).
- [9] L. Avaldi and A. Huetz, *J. Phys. B* **38**, S861 (2005).
- [10] J. S. Briggs and V. Schmidt, *J. Phys. B* **33**, R1 (2000).
- [11] M. S. Schöffler *et al.*, *Phys. Rev. Lett.* **111**, 013003 (2013).
- [12] A. A. Sorokin, M. Wellhöfer, S. V. Bobashev, K. Tiedtke, and M. Richter, *Phys. Rev. A* **75**, 051402(R) (2007).
- [13] A. Rudenko *et al.*, *Phys. Rev. Lett.* **101**, 073003 (2008).
- [14] M. Kurka *et al.*, *New J. Phys.* **12**, 073035 (2010).
- [15] Y. Nabekawa, H. Hasegawa, E. J. Takahashi, and K. Midorikawa, *Phys. Rev. Lett.* **94**, 043001 (2005).
- [16] H. Hasegawa, E. J. Takahashi, Y. Nabekawa, K. L. Ishikawa, and K. Midorikawa, *Phys. Rev. A* **71**, 023407 (2005).
- [17] S. Selstø, X. Raynaud, A. S. Simonsen, and M. Førre, *Phys. Rev. A* **90**, 053412 (2014).
- [18] S. Haessler, J. Caillat, and P. Salieres, *J. Phys. B* **44**, 203001 (2011).
- [19] R. Nepstad, T. Birkeland, and M. Forre, *Phys. Rev. A* **81**, 063402 (2010).
- [20] J. Feist, S. Nagele, R. Pazourek, E. Persson, B. I. Schneider, L. A. Collins, and J. Burgdörfer, *Phys. Rev. A* **77**, 043420 (2008).
- [21] X. Guan, K. Bartschat, and B. I. Schneider, *Phys. Rev. A* **77**, 043421 (2008).
- [22] S. X. Hu, J. Colgan, and L. A. Collins, *J. Phys. B* **38**, L35 (2005).
- [23] J. Colgan and M. S. Pindzola, *Phys. Rev. Lett.* **88**, 173002 (2002).
- [24] S. Laulan and H. Bachau, *Phys. Rev. A* **68**, 013409 (2003).
- [25] B. Piroux, J. Bauer, S. Laulan, and H. Bachau, *Eur. Phys. J. D* **26**, 7 (2003).
- [26] L. A. A. Nikolopoulos and P. Lambropoulos, *J. Phys. B* **34**, 545 (2001).
- [27] L. A. A. Nikolopoulos and P. Lambropoulos, *J. Phys. B* **40**, 1347 (2007).
- [28] E. Fomouo, G. L. Kamta, G. Edah, and B. Piroux, *Phys. Rev. A* **74**, 063409 (2006).
- [29] A. Palacios, D. A. Horner, T. N. Rescigno, and C. W. McCurdy, *J. Phys. B* **43**, 194003 (2010).
- [30] A. Palacios, T. N. Rescigno, and C. W. McCurdy, *Phys. Rev. A* **79**, 033402 (2009).
- [31] D. A. Horner, C. W. McCurdy, and T. N. Rescigno, *Phys. Rev. A* **78**, 043416 (2008).
- [32] D. A. Horner, F. Morales, T. N. Rescigno, F. Martín, and C. W. McCurdy, *Phys. Rev. A* **76**, 030701 (2007).
- [33] I. A. Ivanov and A. S. Kheifets, *Phys. Rev. A* **75**, 033411 (2007).
- [34] A. S. Kheifets and I. A. Ivanov, *J. Phys. B* **39**, 1731 (2006).
- [35] I. A. Ivanov and A. S. Kheifets, *J. Phys. B* **41**, 095002 (2008).
- [36] L. Feng and H. W. van der Hart, *J. Phys. B* **36**, L1 (2003).
- [37] H. W. van der Hart, *Phys. Rev. A* **89**, 053407 (2014).
- [38] M. Kornberg and P. Lambropoulos, *J. Phys. B* **32**, L603 (1999).
- [39] R. Shakeshaft, *Phys. Rev. A* **76**, 063405 (2007).
- [40] H. Bachau, *Phys. Rev. A* **83**, 033403 (2011).
- [41] W.-C. Jiang, W.-H. Xiong, T.-S. Zhu, L.-Y. Peng, and Q. Gong, *J. Phys. B* **47**, 091001 (2014).
- [42] A. Palacios, T. N. Rescigno, and C. W. McCurdy, *Phys. Rev. Lett.* **103**, 253001 (2009).
- [43] D. A. Horner, F. Morales, T. N. Rescigno, F. Martín, and C. W. McCurdy, *Phys. Rev. A* **76**, 030701 (2007).
- [44] D. A. Horner, C. W. McCurdy, and T. N. Rescigno, *Phys. Rev. A* **78**, 043416 (2008).
- [45] A. Palacios, T. N. Rescigno, and C. W. McCurdy, *Phys. Rev. A* **79**, 033402 (2009).
- [46] D. A. Horner, T. N. Rescigno, and C. W. McCurdy, *Phys. Rev. A* **81**, 023410 (2010).
- [47] R. Pazourek, J. Feist, S. Nagele, E. Persson, B. I. Schneider, L. A. Collins, and J. Burgdörfer, *Phys. Rev. A* **83**, 053418 (2011).
- [48] M. Førre, S. Selstø, and R. Nepstad, *Phys. Rev. Lett.* **105**, 163001 (2010); **106**, 129905(E) (2011).
- [49] D. A. Verner, G. J. Ferland, K. T. Korista, and D. G. Yakovlev, *Astrophys. J.* **465**, 487 (1996).
- [50] W.-C. Jiang, Y. Tong, Q. Gong, and L.-Y. Peng, *Phys. Rev. A* **89**, 043422 (2014).
- [51] Z. Zhang, L.-Y. Peng, M.-H. Xu, A. F. Starace, T. Morishita, and Q. Gong, *Phys. Rev. A* **84**, 043409 (2011).
- [52] W.-C. Jiang, L.-Y. Peng, W.-H. Xiong, and Q. Gong, *Phys. Rev. A* **88**, 023410 (2013).
- [53] P. Lambropoulos, L. A. A. Nikolopoulos, M. G. Makris, and A. Mihelic, *Phys. Rev. A* **78**, 055402 (2008).
- [54] J. Berakdar and J. S. Briggs, *Phys. Rev. Lett.* **72**, 3799 (1994).
- [55] M. Brauner, J. S. Briggs, and J. T. Broad, *J. Phys. B* **24**, 287 (1991).
- [56] M. Brauner, J. S. Briggs, and H. Klar, *J. Phys. B* **22**, 2265 (1989).
- [57] M. A. Kornberg and J. E. Miraglia, *Phys. Rev. A* **48**, 3714 (1993).